HHS Public Access

Author manuscript

Gene Ther. Author manuscript; available in PMC 2011 June 01.

Published in final edited form as:

Gene Ther. 2010 December ; 17(12): 1506–1516. doi:10.1038/gt.2010.103.

Mantle cell lymphoma salvage regimen: synergy between a reprogrammed oncolytic virus and two chemotherapeutics

Guy Ungerechts[1], **Marie E Frenzke**[1], **Koon-Chu Yaiw**[1], **Tanner Miest**[1], **Patrick B Johnston**[2], and **Roberto Cattaneo**[1,*]

[1] Department of Molecular Medicine and Virology and Gene Therapy Track, Rochester, MN 55905, USA

[2] Division of Hematology, Mayo Clinic College of Medicine, Rochester, MN 55905, USA

Abstract

MV-PNP H^{blind}antiCD20 is a CD20-targeted and prodrug convertase-armed measles virus (MV) that temporarily controls growth of lymphoma xenografts in SCID mice in combination with fludarabine phosphate. Herein, we examine the replication of this targeted virus and of a vaccine-lineage MV in disease bulks and circulating cells from mantle cell lymphoma (MCL) patients, and show that only the targeted virus is specific for CD20-expressing cells. We then assessed the efficacy of different regimens of administration of this virus in combination with fludarabine and cyclophosphamide (CPA) in a MCL xenograft model. We show that CPA administration before virus enhances oncolytic efficacy, likely through temporary immunosuppression. An interval of one-week between intravenous virus administration and fludarabine treatment further enhanced oncolysis, by synchronizing maximum prodrug convertase expression with fludarabine availability. Finally, three 23-day courses of triple sequential treatment with CPA, virus and fludarabine treatment resulted in complete regression of the xenografts. Secondary disease symptoms interfered with survival, but average survival times increased from 22 to 77 days. These studies document a reprogrammed oncolytic virus consolidating the effects of two chemotherapeutics, a concept well-suited for a phase I clinical trial for MCL patients for whom conventional therapies have failed.

Keywords

cyclophosphamide; fludarabine; mantle cell lymphoma; oncolytic therapy; targeted and armed virus

[*]Corresponding author. Mailing address: Mayo Clinic Rochester, Department of Molecular Medicine, Guggenheim 18-42B, 200 First Street SW, Rochester, MN, 55905, USA, Phone: (507) 284-0171, Fax: (507) 266-2122, Cattaneo.Roberto@mayo.edu.
[#]Present address: National Center for Tumor Diseases (NCT) Heidelberg Im Neuenheimer Feld 350, 69120 Heidelberg, Germany

Conflict of interest Patent applications on which RC is an inventor have been licensed to NISCO, Inc. Mayo has an equity position in NISCO; Mayo has not yet received royalties from products developed by the company, but may receive these in future.

Introduction

Most therapeutic regimens for lymphoma are based on combinations of drugs, radiation and/or surgery to maximize patient survival. Oncolytic viruses are also being combined with other therapeutic modalities: the genetically modified adenovirus H101, which is approved in China for the treatment of head and neck carcinoma, is delivered in combination with chemotherapy [1]. Moreover, several current clinical trials are based on the combination of oncolytic viruses with other therapies [2, 3]. However, current combination regimens rarely achieve synergy between virus and chemotherapy [4]. To maximize therapeutic potential, we sought to reprogram a measles virus (MV) into an oncolytic virus capable of targeting, and enhancing the effects of different chemotherapeutics approved for treatment of lymphoma.

We reasoned that MV might be especially adept to treat lymphoma because of its natural tropism for lymphocytes [5]. Indeed, spontaneous lymphoma [6] and leukemia [7] regressions were repeatedly observed after wild-type MV infection. Moreover, a phase I study of intratumoral (IT) injections of the unmodified MV Zagreb vaccine strain in patients with cutaneous T-cell lymphomas demonstrated safety as well as clinical responses [8]. Pre-clinical studies based on human lymphoma xenografts in immunodeficient mice treated with a vaccine strain MV confirmed strong oncolytic effects [9].

A first line treatment for selected non-Hodgkin lymphoma, as well as the salvage regimen in mantle cell lymphoma (MCL) [10–13], is a combination of the three lymphoma therapeutics fludarabine phosphate (fludarabine), cyclophosphamide (CPA), and the CD20 antibody Rituximab (FCR regimen). To improve on FCR efficacy we generated MV-PNP H^{blind}antiCD20[14], a virus targeted to CD20-expressing cells, blinded to the natural receptors, and armed with the prodrug convertase *E. coli* purine nucleoside phosphorylase (PNP). For infectivity studies, we also generated a similar virus expressing green fluorescent protein (GFP) in place of PNP, and named it MV-GFP H^{blind}antiCD20[14].

Initially, we characterized how the PNP-expressing virus interacts *in vitro* and *in vivo* with fludarabine [14]. Virus-expressed PNP locally activates fludarabine to 2-fluoroadenine, a highly diffusible substance that is metabolized to toxic ATP analogs capable of inhibiting DNA, RNA and/or protein synthesis immediately [15]. In conventional therapy (in the absence of *E. coli* PNP), fludarabine is not metabolized efficiently to 2-fluoroadenine, and thus is not as effective. We also characterized parameters for the safe application of MV-PNP H^{blind}antiCD20 in combination with fludarabine in genetically modified mice susceptible to MV infection, and showed that virus plus fludarabine temporarily control growth of Burkitt (Raji cells) and MCL (Granta cells) lymphoma xenografts in SCID mice [14].

Herein, we compared the replication of the CD20-targeted and vaccine-lineage MV in primary lymphoma cells from MCL patients, and showed that only the targeted virus is strongly specific for CD20-expressing lymphoma cells. In anticipation of moving toward a phase I clinical trial, we also sought to treat MCL xenografts established in SCID mice. We administered CPA before virus treatment to establish immunosuppression and enhance virus replication, resulting in increased oncolytic efficacy. We then optimized dosing and scheduling for CPA, MV-PNP H^{blind}antiCD20, and fludarabine, and defined the interval

between virus and fludarabine application that produced the strongest oncolytic effect. Different types of cyclic treatment were also tested, one of which more than tripled survival time.

Results

CD20-targeting of MV to primary lymphoma cells of MCL patients

To assess in clinical samples the level of specificity conferred to MV by targeting to CD20, we used tumor biopsies or peripheral blood mononuclear cells (PBMC), including circulating lymphoma cells, from MCL patients. These samples were divided in aliquots that were infected either with the GFP-expressing virus MV-GFP H^{blind}antiCD20[14], or a control vaccine-lineage virus with the same CD46 receptor specificity of the MV currently used in clinical trials [16], [17], or mock-infected.

Figure 1 shows an analysis of the levels of infection of CD20-positive and CD20-negative PBMC from three patients. At a multiplicity of infection (m.o.i.) of 1, the vaccine-lineage MV (MV-GFP) infected efficiently both cell populations of all three patients (28–65% infected cells Figure 1A–C, right upper and lower panels). At the same m.o.i., MV-GFP H^{blind}antiCD20 infected about 30% of the CD20-positive cells of patients A and B, but only about 4 or 7% of the CD20-negative cells of these patients, respectively (Figure 1A, second from right panels, and Figure 1B, left panels). Thus CD20-expressing cells of patients A and B were infected approximately 7 and 5 times more efficiently than the CD20-negative cells. However, the ratio of infection of the CD20-positive and negative cells of patient C was close to 1 (Figure 1C, compare left pair of panels and right pair of panels). Thus, we performed additional comparative infection analyses in PBMC or in spleen biopsies from eight different MCL patients. Analyses of these samples confirmed heterogeneity of specific infection ratios: about 4-to 6-fold preferential infection was documented in samples from three patients, 2-fold preferential infection in other three samples, and no specificity in two samples. Five times higher multiplicity of infection enhanced the percentile of infected cells 1.5–5 times but did not alter infection ratios (data not shown). Thus, 2- to 7-fold enhanced CD20 specificity of the retargeted virus was documented in 8 of 11 patient's samples.

Systemic treatment with virus and fludarabine reduces primary tumor burden

We previously documented that IT inoculation of the PNP-armed version of the CD20-targeted virus (MV-PNP H^{blind}antiCD20) is effective in the treatment of Granta 519 MCL xenografts in SCID mice [14]. Since IT therapy is of limited value for the treatment of a disseminated malignancy like MCL, we injected the virus via tail vein with or without subsequent intraperitoneal (IP) fludarabine administration. We assessed oncolytic efficacy of systemic virus administration by measuring the volume of subcutaneously implanted xenografts over time.

As in our previous study, treatment started when subcutaneous MCL tumors reached an average volume of 20–40 μl. Groups of 9 mice were treated with virus alone (five doses in consecutive days), low levels of fludarabine alone (three doses in consecutive days), a combination of virus and fludarabine (first dose of fludarabine administered one day after

the last dose of virus), or left untreated (mock-treatment). The mean of the tumor volume in each group of mice measured each third day over a 27-day period is shown in Figure 2A. The tumor volume in individual mice at day 24 post-treatment is shown in Figure 2B.

As expected, fludarabine had a small but significant therapeutic effect; a moderate reduction of tumor volume was documented in the fludarabine only treated mice compared to the mock-treated group (Fig. 2A and 2B, compare diamonds and squares, p=0.01 at day 24). In contrast, the mean tumor volume in the groups treated with either virus alone (Fig. 2A and 2B, triangles) or with both virus and prodrug (Fig. 2A and 2B, dots) was strongly reduced compared to mock-treatment. Furthermore, there is a significant decrease in tumor volume with combination therapy compared to virus alone (Fig. 2B, p=0.0424 at day 24).

The tumor volumes measured in individual mice 27 days after start of treatment were as follows: all but one of the nine mock-treated mice had been sacrificed due to tumor burden (>1700 μl). Seven of the nine mice treated with fludarabine had tumors ranging in size from 787 to 1690 μl, one was sacrificed, and one tumor regressed. Seven of eight mice treated with virus alone had tumors ranging in size from 256 to 1267 μl, and one tumor regressed. Five of nine combination-treated mice had tumors ranging in size from 48 to 600 μl, with four tumor regressions. Altogether, these data show that intravenous (IV) treatment with virus followed by fludarabine administration is effective in initially reducing the primary tumor volume. However, the xenografts eventually resumed growing.

Fludarabine administration one week after virus delivery is most effective

Timing of prodrug administration after IV virus delivery can be critical, as previously documented for an armed adenovirus [18]. In an empiric attempt to synchronize prodrug delivery with high levels of virus replication, we extended the time window between virus inoculation and fludarabine delivery. In another experiment, the first treatment group received fludarabine on days 5, 6 and 7 after the first virus administration (Fig. 3A, open circles, group F1 timing), as done in our initial experiment. The second and third treatment groups received fludarabine at days 12, 13 and 14 after the first virus administration (Fig. 3A, open squares, group F2 timing) or at days 19, 20 and 21 thereafter (Fig. 3A, open diamonds, group F3 timing). Maximum efficiency of oncolysis was achieved with the schedule F2: two-sample t-test of pair-wise comparison of this group of mice with the MV-only group on day 15 yielded a significant value of p=0.02. The F1-MV-only comparison and F3-MV-only comparison yielded the non-significant values of p=0.14 and p=0.6, respectively. Accordingly, all mice in the F2 treatment group were alive 33 days post tumor implantation (Fig. 3B, open squares), while most mice in the F1 and F2 treatment groups had already been sacrificed. Thus, we selected the one-week time interval for fludarabine administration in subsequent experiments.

CPA administration one day before infection improves oncolytic efficacy

CPA is one component of the FCR regimen, but it is also an immunosuppressant that acts both on acquired and innate immunity. We and others have previously taken advantage of the immunosuppressive property of CPA to enhance MV replication in toxicity [19] and

efficacy [20] studies of oncolytic therapy in immunocompetent models. CPA was also shown to inhibit the innate immune response in oncolysis protocols using other viruses [21], [22].

We therefore assessed whether administration of an appropriate dose of CPA enhances oncolytic efficacy in the SCID xenograft model, in which acquired immune responses are minimal. To limit the direct anti-tumor effects of the cytoreductive agent CPA, which occur through DNA alkylation, we treated mice bearing subcutaneous MCL xenografts with doses of 25, 50, or 100 mg CPA/kg. Figure 4A shows the time course of tumor growth in different experimental groups, and Figure 4B shows the tumor volumes in individual mice 18 days after CPA administration. Treatment with 25 mg/kg (Fig. 4A and 4B, triangles) had no effect on tumor growth, producing an overlapping growth curve with the negative control (Fig. 4A and 4B, mock, squares). Treatment with 50 mg/kg (Fig. 4A and 4B, dots) had a limited effect on tumor growth that was not significant ($p=0.0551$ compared to mock treatment), whereas treatment with 100 mg/kg retarded tumor growth significantly (Fig. 4A and 4B, diamonds; $p=0.0019$ compared to mock treatment). Since our goal was to limit the direct anti-tumor effect of CPA, allowing potential effects of virus therapy to manifest, the intermediate dose (50 mg/kg) was selected for subsequent experiments.

Triple treatment chemovirotherapy: CPA, virus and fludarabine

We then assessed the efficacy of a triple treatment regimen for MCL combining the clinically approved components CPA and fludarabine with our armed and targeted virus. We used the optimal concentration and timing parameters determined in the experiments above: a single IP injection of CPA (50 mg/kg), or control saline, at day -1 followed by five IV injections of 10^6 infectious units of virus, or mock-infection, at days 0–4. Groups of mice treated with fludarabine received three IP injections (250 mg/kg/dose) at days 12–14.

The kinetic analysis of tumor growth was done in groups of 10–12 mice and is shown in Figure 5A. Tumor volume data from all individual mice in each group are shown in Figure 5B at day 20 after start of viral treatment. CPA application alone (filled triangles) only marginally slowed tumor growth as compared to saline (filled squares), and this effect occurred in the first days of treatment. Treatment with virus alone (filled circles) retarded tumor growth more markedly, and this effect was evident ten days after virus application, suggesting an important role for virus replication. Treatment with virus and CPA (open triangles) appeared to be initially more effective than treatment with either individual component, and was significantly different from virus alone on day 20 of the experiment ($p=0.0177$, Figure 5B). Treatment with virus and fludarabine (open circles) seemed slightly more effective than treatment with virus and CPA, and tumor volume on day 20 was significantly lower ($p=0.0077$, Figure 5B). Finally, combination of all three therapeutics (open squares) reduced tumor burden significantly better than any other treatment (day 20, $p=0.0002$ as compared to virus alone). However, a single round of this combination therapy did not eliminate the tumor.

The percentile of tumor cells circulating in the blood of mice on day 25 was also examined systematically as a second parameter of treatment efficacy. Remarkably, a significant decrease in circulating MCL cells was seen in all virus-treated mice when compared to mock-treated animals (Fig. 5C). While PBMC of mock-treated mice averaged

approximately 11 % tumor cells (left column) only very few (about 1 % or less) tumors cells were detected in the blood of virus-treated animals (third to sixth column). Thus virus treatment was particularly effective at reducing the number of circulating tumor cells.

Repeated sequential treatment with CPA, virus and fludarabine eliminates implanted tumors and prolongs survival

In clinical practice, lymphoma therapy is typically based on sequential administration of multiple cycles of therapy. To obtain *in vivo* data towards a clinical trial for the treatment of MCL patients, we compared different schedules of sequential delivery of virus and chemotherapeutics on the growth of MCL tumors in SCID mice. Figure 6A (bottom) illustrates these schedules. The triple treatment (top line, triangles) is a control repetition of the one cycle treatment from Figure 5. The triple+2F treatment (second line, diamonds) consists of treatment with CPA, virus and three cycles of treatment with fludarabine. The triple-triple treatment (third line, squares) consists of three repetitions of the cycle of three therapeutics. Mock-treatment (dots) served as control.

The triple treatment slowed tumor growth (Fig. 6A, compare triangles with dots), extending survival to average 41 days (Kaplan-Meier curve of Fig. 6B, compare triangles with circles) but was unable to completely control tumor growth. Nine of the 11 mice treated had to be sacrificed 38–47 days after beginning of treatment, whereas all 10 untreated mice had to be sacrificed at days 20–26 (average survival: 23 days). The triple+2F treatment (Fig. 6A and 6B, diamonds; average survival: 51.5 days) slowed tumor growth and extended survival slightly more efficiently than the triple treatment.

The triple-triple treatment was clearly most effective: a few days after the second cycle of virus delivery, tumour growth slowed and was controlled (Fig. 6A, squares). Statistical analysis performed in the third month of treatment indicated highly significant tumor volume differences between this and the other treatments ($p=0.0004$ compared to triple treatment; $p=0.0038$ compared to triple+2F). Simultaneously with the third cycle of virus delivery, the volume of most tumors began to shrink. However, while the subcutaneously implanted tumors were disappearing, several mice developed complications and all mice had to be sacrificed at days 70–80 (average survival: 77 days, Fig. 6B, squares).

Causes of morbility and mortality

The symptoms noted in individual mice in all four experimental groups are listed in the three left columns of Table I; pathological findings at autopsy are listed in the four columns on the right. Several mice showed signs of systemic disease including wasting, leg paralysis, ascites, labored breathing, a hunched posture and body tremors. These symptoms were detected only in the treatment groups because all non-treated animals had to be sacrificed early. With one exception, symptoms started after day 35, and 13 of 17 symptom-related deaths were after day 49. On necropsy therapy-refractory tumors were diagnosed in the abdomen and/or thorax or in inguinal and axillary lymph nodes. Spleens were enlarged in all treatment groups except group 3, which had the smallest implanted tumor weights, the lowest average increase in lymph node weight, but also the largest increase in the weight of new therapy-resistant tumors. These observations suggest that implanted tumors, but not

secondary tumors, were well controlled by therapy. To assess whether secondary tumors had reduced CD20 expression levels, tumors were analyzed by immunohistochemistry, but there were no obvious differences in the levels of expression between the primary and secondary tumors.

To assess whether tumor cells were circulating during early and late phases of infection, blood smears were done at day 21, and then again at autopsy. The day 21 analyses showed that the mock-treated group averaged about 10% circulating tumor cells in the PBMC, whereas the three treatment groups all averaged only 1–2% circulating tumor cells (1.8, 1.4 and 1.4% for groups 1, 2 and 3, respectively, data not shown). At the time of necropsy, however, average percentage of tumor cells in PBMC in experimental groups was in the same range as in the non-treated group. Thus the three complete cycles of chemotherapy and virus treatment often resulted in complete elimination of the implanted tumor, but failed to control secondary tumors and circulating MCL cells.

Discussion

Targeting efficacy in clinical samples

Translation of promising results from the bench to the bedside is challenging, and the excitement of providing new therapies for otherwise incurable cancer is often countered by loss of efficacy *in vivo*, and safety concerns. Targeting has great potential for enhancing safety and potency of new therapeutic modalities, but its efficacy must be proven in patient's materials and in animal systems. We show here that a vaccine-lineage MV with CD46 receptor specificity infects spleen disease bulks and PBMC of MCL patients with roughly the same efficiency as it infects the stable cell line used to propagate it. However, this virus infects with similar efficiency CD20-expressing lymphoma cells and non CD20-expressing normal immune cell types including T-lymphocytes.

In contrast, MV-PNP H^{blind}antiCD20 shows enhanced specificity for CD20-expressing cells from MCL patients infecting CD20-positive lymphoma cells 2–7 times more efficiently than CD20-negative cells. This level of specificity is less pronounced in lymphoma cells than in PBMC of healthy individuals, where we measured a 10-fold higher infectivity in CD20-positive than in CD20-negative cells (K.-C.Y., M.F., and R.C., unpublished), or than in cultivated cells, where 40- to 100-fold specificity gains have been documented [23], [24]. Even if, by the above criteria, the 2- to 7-fold gain in specific cell entry and viral replication documented here in most clinical samples seems small, this gain can be of critical importance. However, complete lack of CD20-specificity in clinical samples of 3 of 11 patients was also documented. This was unexpected and is not yet understood, but may be due to complicating variables such as therapy received prior to obtaining patient samples. These data argue for comparing the replication of MV-PNP H^{blind}antiCD20 and vaccine-lineage MV in individual samples before considering inclusion of a patient in a MCL clinical trial based on a retargeted therapeutic virus.

Delivery schedule

In addition to quantifying targeting efficiency in clinical samples, we sought to develop an effective pre-clinical protocol for timing the delivery of MV-PNP H^{blind}antiCD20 in combination with fludarabine and CPA. Combination therapies with oncolytic viruses require accurate timing because viruses need to replicate in target cells before developing their full synergistic potential with chemotherapeutics. Viruses armed with convertases that toxify a substrate can poison the host cell suddenly, effectively arresting viral spread. We previously characterized parameters for the safe application of MV-PNP H^{blind}antiCD20 in combination with only fludarabine in genetically modified mice susceptible to MV infection [14].

The sequence and timing of administration and dosage of these three components was planned based on results from previous experimentation with MV and other oncolytic viruses [20–22]. We reasoned that the appropriate sequence was administration of CPA, followed by virus, and finally fludarabine. Indeed, a single CPA dose applied IP one day before beginning IV virus treatment enhanced oncolytic efficacy, likely by suppressing host innate and adaptive immunity and favoring virus replication, as observed with other oncolytic viruses [25–27]. We then optimized the time window between virus application and fludarabine treatment: the initial empirical treatment schedule was based on fludarabine administration one day after the last virus dose [14], but a study with an armed adenovirus [18] showed that increasing the interval between infection and prodrug administration improved therapeutic efficacy. Here we show that the most effective time point for fludarabine administration was one week after the last virus injection. Thus the optimal sequence of delivery is CPA on day -1, virus on days 0–4, and fludarabine on days 12–14. The third improvement was repetition of the 23-day course of sequential treatment with CPA, virus and fludarabine; three repetitions consistently caused complete regression of the implanted tumors.

Proposed MCL clinical trial

Our data compare favorably with pre-clinical studies of a reagent currently in phase 1 clinical trials, the therapeutic HLA-DR-specific monoclonal antibody 1D09C3[28]. Repeated IV administration of this antibody to SCID mice with implanted Granta 519 cell xenografts was less effective than the above described treatment regimen including CPA, virus and fludarabine. In the experiments with 1D09C3 long-term survival at day 50 after tumor implantation was only 80 % and there was no complete remission within the observation period of 46 days. A further pre-clinical study with MCL-bearing SCID mice demonstrated synergistic effects of the proteasome inhibitor bortezomib, the anti-CD20 antibody Rituximab and CPA (BRC regimen) with a therapeutic outcome similar to that described in our study with 70 % long-term survival at day 70 post-tumor implantation and complete remission of subcutaneous tumors [29]. Thus our pre-clinical efficacy data support the development of a clinical protocol, especially when it is noted that the side effects that interfered with survival in our animal models can often be successfully controlled in patients.

We are designing a phase I clinical trial to test the safety of MV-PNP H^{blind}antiCD20 in combination with fludarabine and CPA, to be named FCV for fludarabine, CPA and virus. MCL patients who fail chemo- and radiation therapy will be recruited. The new salvage regimen will be based on the sequence and timing of delivery of the reagents tested in the above pre-clinical experiments. Current FCR clinical regimens administer Rituximab (375 mg/m^2) on day 1 and cyclophosphamide (250 mg/m^2) and fludarabine (25 mg/m^2) on days 2–4. The cycle is completed by 24 days of rest and is repeated up to 6 times. A comparable FCV course would consist of a single administration of cyclophosphamide (375 mg/m^2, half the total dose administered over 3 days in the FCR regimen) on day 1, administration of the virus in a dominant node on day 2, one week of rest, fludarabine administration (25 mg/m^2) on days 10–12, and two weeks of rest. This course will be repeated up to six times. We are aware of possible toxic effects of this combination treatment; since slow leukocyte and platelet recovery often necessitate delays in administration and dose reductions in the FCR regimen, we would propose a step-wise reduction in fludarabine in response to toxicity. Side effects in a clinical trial based on the FCV regimen may be aided by experience gained from patients treated with the FCR regimen [30].

Systemic treatment of patients with high MV-neutralizing antibodies titers remains a challenge. Two MV-based clinical trials currently open (ovarian carcinoma and glioma) depend on local virus administration, and a third trial using systemic delivery treats myeloma patients with low titers of MV antibodies [31]. Even when no antibodies are present, the first injection of an oncolytic virus will induce neutralizing antibodies that can quench the activity of subsequent injections. To avoid neutralization, other viral systems have used the envelopes of different serotypes are used sequentially [32]. Since re-coating with alternative serotypes is not possible for MV, which is monotypic, we have used the envelope proteins of canine distemper virus to shield MV from neutralizing antibodies (K.-C. Y., J. Lampe, G.U. and R.C., unpublished data), and vice-versa [33]. Moreover, we are generating a chimeric virus with the re-targeted envelope glycoproteins of another paramyxovirus [34]. Thus, re-targeted viruses capable of escaping neutralization may soon be available for more effective consecutive cycles of systemic therapy.

Materials and methods

Viruses

Two CD20-targeted MV, one armed PNP and named MV-PNP H^{blind}antiCD20, the other expressing GFP from the same additional transcription unit and named MV-GFP H^{blind}antiCD20, were previously generated in our laboratory [14]. To prepare stocks, Vero-αHis cells [35] were infected (multiplicity of infection of 0.03) and incubated at 37°C for 36 h. Virus was harvested by one freeze-thaw cycle and resuspended in Opti-MEM (Invitrogen, Grand Island, NY). Titers were determined by 50% tissue culture infectious dose ($TCID_{50}$) titration by the method of Karber [36] on Vero-αHis cells.

Patient's samples

This project utilized samples of blood and tumor tissue from MCL patients obtained through a NCI Lymphoma SPORE grant awarded to University of Iowa-Mayo Clinic; protection of human subjects was as approved by the Institutional Review Board.

Primary MCL cells were recovered from fresh blood or surgically removed spleen tissue. When cell were recovered from spleen, fresh tissue was cut up and minced over an 80 μm wire mesh to obtain a single cell suspension, which was overlaid on Ficoll-Paque Plus (GE Healthcare Piscataway, NJ) and centrifuged to isolate the mononuclear cell layer. Fresh whole blood was collected in EDTA tubes (Becton Dickinson, Franklin Lakes, NJ) and subjected to Ficoll-Hypaque (GE Healthcare, Piscataway, NJ) density gradient centrifugation as above. The cell layer was then collected, washed twice with Hank's buffered saline solution (Mediatech, Manassas, VA), counted, and 5×10^4 cells per well were seeded on 24-well plate in RPMI 1640 (Mediatech, Manassas, VA) supplemented with 10% fetal calf serum (FCS) and antibiotics.

Infection of patient's materials and flow cytometry analyses

The cells were then infected at a m.o.i. of 1 (5×10^4 $TCID_{50}$) with either MV-GFP H^{blind}antiCD20[14] or MV-GFP (also named MVgreen) [37]. Forty-eight hours post infection, cells were harvested and washed twice with washing buffer: 5% FCS, 0.05% sodium azide in phosphate buffered saline (PBS). Cells were labeled using PE CD20 (BD Bioscience; 10 μl/test; catalogue number (cat): 555623), PerCP CD45 (BD Bioscience; 5 μl/test; cat: 340665) and in some cases APC CD3 (BD Bioscience; 15 μl/test; cat: 557597) for 1.5 hours in the dark at 4°C. The respective isotype controls were also included in every test, along with mock-infected cells. Cells were then washed twice with washing buffer, followed by final wash with 5% FCS in PBS and fixed in 1% paraformaldehyde in PBS before performing fluorescence-activated cell sorting (FACS) analysis (FACSCalibur, BD Biosciences).

Compensation with single tube color was done on each sample in duplicate before each test run. A total of 10,000 events were acquired and analyzed using FACSDiva software (BD Bioscience). Live CD45+ lymphocytes were gated according to the forward and side scatters properties. The CD45+ population was further gated for CD20+ and CD20− populations, and GFP signal within each population was used to determine virus infectivity in each sub-population. The mean CD20 fluorescence intensity was determined on patient's samples, but there was no correlation with levels of infection.

Cell culture

MCL cells (Granta 519) [38], and Vero-αHis cells [35] were grown at 37°C in a humidified atmosphere of 5% CO_2 either in RPMI with 10% FCS (Invitrogen, Grand Island, NY) or in Dulbecco's Modification of Eagles's Medium (DMEM) (Mediatech Inc., Herndon, VA) with 10% FCS, respectively.

Establishment of subcutaneous tumors

Experimental protocols were approved by the Institutional Animal Care and Use Committee. Tumors were established by inoculating Granta 519 cells (10^7/100μl per site) subcutaneously into the right flanks of 6–8 week old SCID mice (Harlan).

Tumor treatment with virus, fludarabine or CPA

When tumors measured an average of 20–40 μl, the treatment regimens were initiated. Virus (MV-PNP H^{blind}antiCD20) was injected in the tail vein at 1×10^6 infectious units in 100μl Opti-MEM per dose for 5 consecutive days. Control animals were injected intravenously (IV) with equal volumes of Opti-MEM containing no virus. Intratumoral (IT) injections were as described [14].

Fludarabine (phosphate for injection) (SICOR Pharmaceuticals, Irvine, CA) was reconstituted with sterile H_2O as per manufacturer. Mice receiving fludarabine were injected with 250 mg/kg body weight/dose intraperitoneally (IP) each day for 3 consecutive days.

CPA (Cytoxan for injection) (Bristol-Myers Squibb, Princeton, NJ) was reconstituted with sterile H_2O as per manufacturer. When tumors measured an average of 20–40 μl, mice were treated with a single intraperitoneal injection of saline or CPA (25, 50, or 100 mg/kg body weight).

Measurements of tumor volume

Tumor diameters were measured every 3rd day and the estimated volume (product of 0.5 × longest diameter × $width^2$) was indicated as mean ± standard error of mean (s.e.m.) for each group. Animals were sacrificed when their tumor burden reached a volume of about 10% of body weight (about 1700 μl). Treatment of the mice was halted if they lost 15% of their body weight, or they developed severe symptoms of distress.

Blood collection from mice, and analysis

Samples of blood (50–200μl) were taken by cheek bleed and collected in lithium heparin tubes (Becton Dickinson, Franklin Lakes, NJ). Most samples were analyzed by microscopy. Blood smears were prepared and stained with Wright-Giemsa (Sigma-Aldrich, St. Louis, MO) (as per manufacturer). Standard differential white blood cell (WBC) counts were done and slides were examined for the presence of circulating Granta 519 cells. The percentage of Granta 519 cells per total WBC was determined. In addition, some samples were analyzed by FACS. A PE labeled anti-human CD19 antibody and a PE labeled isotype control (Becton Dickinson, Franklin Lakes, NJ) were used. Flow cytometric analysis was done using the (FACSCalibur, BD Biosciences) with Cell Quest software (Becton Dickinson).

Complications

Mice receiving repeated cycles of treatments with CPA, virus and fludarabine often cleared the implanted tumors but presented disseminated tumors and secondary disease signs. These included leg paralysis (an inability to extend or contract a leg – usually occurring with the rear legs), ascites (fluid in the abdominal cavity – usually noted by abdominal extension), hunched posture (a relatively inactive state in which the animal is in a fixed position with a

highly arched back), wasting (visible loss of body fat and muscle mass – actual weight loss may be masked by increased tumor volume), body tremors (mice display twitching or jerking motions, particularly in the upper half of the body), labored breathing (mice are less active, appear to have strained breaths and prominent heartbeats).

Necropsies

For necropsies, tissues were collected in 10% (w/v) buffered formalin (Fisher Scientific, Kalamazoo, MI). Sections of tissue were embedded in paraffin, cut, and stained with hematoxylin and eosin.

Statistical analyses

Data were analyzed by using the ANOVA test to compare the treatment groups for tumor volume analysis. The 2-sample t-test was used to make pair-wise comparisons between the treatment groups. Survival data were analyzed by the Kaplan-Meier method and the log-rank test was used to test for significance between all the groups. Since only mice that were sacrificed due to maximum tumor volume were analyzed, the 2-sample t-test was also used to make pair-wise comparisons between the groups. P-values < 0.05 were considered statistically significant.

Acknowledgments

This work was supported by a grant of the Alliance for Cancer Gene Therapy, NIH grant R01 CA139389, and by grant UN 254 1-1 of the Deutsche Forschungsgemeinschaft (German Research Foundation). We thank Johanna Lampe for excellent support, Mary Stenson and Tammy Rattle for the FACS analyses and help with the patient's samples, Mary Bennett for excellent secretarial assistance, Steve Russell and Christof von Kalle for comments on the manuscript.

References

1. Garber K. China approves world's first oncolytic virus therapy for cancer treatment. J Natl Cancer Inst. 2006; 98:298–300. [PubMed: 16507823]
2. Liu TC, Galanis E, Kirn D. Clinical trial results with oncolytic virotherapy: a century of promise, a decade of progress. Nat Clin Pract Oncol. 2007; 4:101–117. [PubMed: 17259931]
3. Patel P, Young JG, Mautner V, Ashdown D, Bonney S, Pineda RG, et al. A phase I/II clinical trial in localized prostate cancer of an adenovirus expressing nitroreductase with CB1984. Mol Ther. 2009; 17:1292–1299. [PubMed: 19367257]
4. Ottolino-Perry K, Diallo J-S, Lichty BD, Bell JC, McCart JA. Intelligent design: combination therapy with oncolytic viruses. Mol Ther. 2010; 18:251–263. [PubMed: 20029399]
5. Cattaneo R, Miest T, Shashkova EV, Barry MA. Reprogrammed viruses as cancer therapeutics: targeted, armed and shielded. Nat Rev Microbiol. 2008; 6:529–540. [PubMed: 18552863]
6. Bluming AZ, Ziegler JL. Regression of Burkitt's lymphoma in association with measles infection. Lancet. 1971; 2:105–106. [PubMed: 4103972]
7. Pasquinucci G. Possible effect of measles on leukaemia. Lancet. 1971; 1:136. [PubMed: 4099624]
8. Heinzerling L, Kunzi V, Oberholzer PA, Kundig T, Naim H, Dummer R. Oncolytic measles virus in cutaneous T-cell lymphomas mounts antitumor immune responses in vivo and targets interferon-resistant tumor cells. Blood. 2005; 106:2287–2294. [PubMed: 15961518]
9. Grote D, Russell SJ, Cornu TI, Cattaneo R, Vile R, Poland GA, et al. Live attenuated measles virus induces regression of human lymphoma xenografts in immunodeficient mice. Blood. 2001; 97:3746–3754. [PubMed: 11389012]

10. Schulz H, Klein SK, Rehwald U, Reiser M, Hinke A, Knauf W-U, et al. Phase 2 study of a combined immunochemotherapy using rituximab and fludarabine in patients with chronic lymphocytic leukemia. Blood. 2002; 100:3115–3120. [PubMed: 12384407]
11. Elter T, Hallek M, Engert A. Fludarabine in chronic lymphocytic leukaemia. Expert Opin Pharmacother. 2006; 7:1641–1651. [PubMed: 16872267]
12. Witzig TE. Current treatment approaches for mantle-cell lymphoma. J Clin Oncol. 2005; 23:6409–6414. [PubMed: 16155027]
13. Jares P, Colomer D, Campo E. Genetic and molecular pathogenesis of mantle cell lymphoma: perspectives for new targeted therapeutics. Nat Rev Cancer. 2007; 7:750–762. [PubMed: 17891190]
14. Ungerechts G, Springfeld C, Frenzke ME, Lampe J, Johnston PB, Parker WB, et al. Lymphoma chemovirotherapy: CD20-targeted and convertase-armed measles virus can synergize with fludarabine. Cancer Res. 2007; 67:10939–10947. [PubMed: 18006839]
15. Parker WB, Allan PW, Shaddix SC, Rose LM, Speegle HF, Gillespie GY, et al. Metabolism and metabolic actions of 6-methylpurine and 2-fluoroadenine in human cells. Biochem Pharmacol. 1998; 55:1673–1681. [PubMed: 9634004]
16. Galanis E, Hartmann LC, Cliby WA, Long HJ, Peethambaram PP, Barrette BA, et al. Phase I trial of intraperitoneal administration of an engineered strain of measles virus modified to express carcinoembryonic antigen for recurrent ovarian cancer. Cancer Res. 2010; 70:875–882. [PubMed: 20103634]
17. Navaratnarajah CK, Leonard VHJ, Cattaneo R. Measles virus glycoprotein complex assembly, receptor attachment and cell entry. Curr Top Microbiol Immunol. 2009; 329:59–76. [PubMed: 19198562]
18. Seo E, Abei M, Wakayama M, Fukuda K, Ugai H, Murata T, et al. Effective gene therapy of biliary tract cancers by a conditionally replicative adenovirus expressing uracil phosphoribosyltransferase: significance of timing of 5-fluorouracil administration. Cancer Res. 2005; 65:546–552. [PubMed: 15695398]
19. Myers RM, Greiner SM, Harvey ME, Griesmann G, Kuffel MJ, Buhrow SA, et al. Preclinical pharmacology and toxicology of intravenous MV-NIS, an oncolytic measles virus administered with or without cyclophosphamide. Clin Pharmacol Ther. 2007; 82:700–710. [PubMed: 17971816]
20. Ungerechts G, Springfeld C, Frenzke ME, Lampe J, Parker WB, Sorscher EJ, et al. An immunocompetent murine model for oncolysis with an armed and targeted measles virus. Mol Ther. 2007; 15:1991–1997. [PubMed: 17712331]
21. Fulci G, Breymann L, Gianni D, Kurozomi K, Rhee SS, Yu J, et al. Cyclophosphamide enhances glioma virotherapy by inhibiting innate immune responses. Proc Natl Acad Sci U S A. 2006; 103:12873–12878. [PubMed: 16908838]
22. Di Paolo NC, Tuve S, Ni S, Hellstrom KE, Hellstrom I, Lieber A. Effect of adenovirus-mediated heat shock protein expression and oncolysis in combination with low-dose cyclophosphamide treatment on antitumor immune responses. Cancer Res. 2006; 66:960–969. [PubMed: 16424031]
23. Vongpunsawad S, Oezgun N, Braun W, Cattaneo R. Selectively receptor-blind measles viruses: identification of residues necessary for SLAM- or CD46-induced fusion and their localization on a new hemagglutinin structural model. J Virol. 2004; 78:302–313. [PubMed: 14671112]
24. Leonard VHJ, Hodge G, Reyes-del Valle J, McChesney MB, Cattaneo R. Signaling lymphocytic activation molecular (SLAM, CD150)-blind measles virus is attenuated and induces strong adaptive immune responses in rhesus monkeys. J Virol. 2010; 84:3280–3286. [PubMed: 20032173]
25. Li H, Zeng Z, Fu X, Zhang X. Coadministration of a herpes simplex virus-2 based oncolytic virus and cyclophosphamide produces a synergistic antitumor effect and enhances tumor-specific immune responses. Cancer Res. 2007; 67:7850–7855. [PubMed: 17699791]
26. Fulci G, Dmitrieva N, Gianni D, Fontana EJ, Pan X, Lu Y, et al. Depletion of peripheral macrophages and brain microglia increases brain tumor titers of oncolytic viruses. Cancer Res. 2007; 67:9398–9406. [PubMed: 17909049]

27. Qiao J, Wang H, Kottke T, White C, Twigger K, Diaz RM, et al. Cyclophosphamide facilitates antitumor efficacy against subcutaneous tumors following intravenous delivery of reovirus. Clin Cancer Res. 2008; 14:259–269. [PubMed: 18172278]
28. Nagy ZA, Hubner B, Lohning C, Rauchenberger R, Reiffert S, Thomassen-Wolf E, et al. Fully human, HLA-DR-specific monoclonal antibodies efficiently induce programmed death of malignant lymphoid cells. Nat Med. 2002; 8:801–807. [PubMed: 12101408]
29. Wang M, Han XH, Zhang L, Yang J, Qian JF, Shi YK, et al. Bortezomib is synergistic with rituximab and cyclophosphamide in inducing apoptosis of mantle cell lymphoma cells in vitro and in vivo. Leukemia. 2008; 22:179–185. [PubMed: 17898787]
30. Tam CS, O'Brien S, Wierda W, Kantarjian H, Wen S, Do K-A, et al. Long-term results of the fludarabine, cyclophosphamide, and rituximab regimen as initial therapy of chronic lymphocytic leukemia. Blood. 2008; 112:975–980. [PubMed: 18411418]
31. Msaouel P, Dispenzieri A, Galanis E. Clinical testing of engineered oncolytic measles virus strains in the treatment of cancer: an overview. Curr Opin Mol Ther. 2009; 11:43–53. [PubMed: 19169959]
32. Rose NF, Marx PA, Luckay A, Nixon DF, Moretto WJ, Donahoe SM, et al. An effective AIDS vaccine based on live attenuated vesicular stomatitis virus recombinants. Cell. 2001; 106:539–549. [PubMed: 11551502]
33. von Messling V, Zimmer G, Herrler G, Haas L, Cattaneo R. The hemagglutinin of canine distemper virus determines tropism and cytopathogenicity. J Virol. 2001; 75:6418–6427. [PubMed: 11413309]
34. Springfeld C, von Messling V, Tidona CA, Darai G, Cattaneo R. Envelope targeting: hemagglutinin attachment specificity rather than fusion protein cleavage-activation restricts Tupaia paramyxovirus tropism. J Virol. 2005; 79:10155–10163. [PubMed: 16051808]
35. Nakamura T, Peng KW, Harvey M, Greiner S, Lorimer IA, James CD, et al. Rescue and propagation of fully retargeted oncolytic measles viruses. Nat Biotechnol. 2005; 23:209–214. [PubMed: 15685166]
36. Kärber G. Beitrag zur kollektiven Behandlung pharmakologischer Reihenversuche. Arch Exp Pathol Pharmakol. 1931; 162:480–483.
37. Schneider U, von Messling V, Devaux P, Cattaneo R. Efficiency of measles virus entry and dissemination through different receptors. J Virol. 2002; 76:7460–7467. [PubMed: 12097558]
38. Jadayel DM, Lukas J, Nacheva E, Bartkova J, Stranks G, De Schouwer PJ, et al. Potential role for concurrent abnormalities of the cyclin D1, p16CDKN2 and p15CDKN2B genes in certain B cell non-Hodgkin's lymphomas. Functional studies in a cell line (Granta 519). Leukemia. 1997; 11:64–72. [PubMed: 9001420]

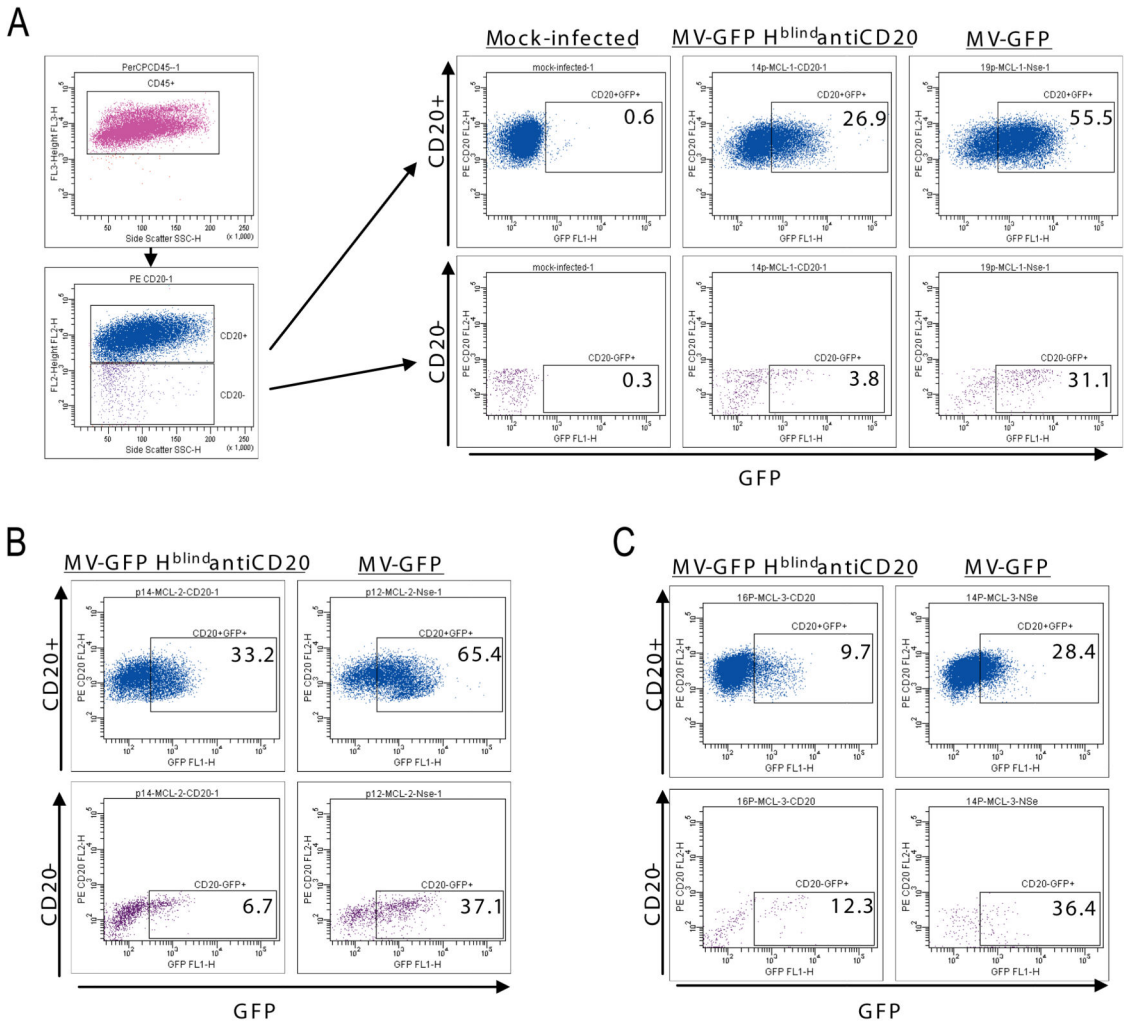

Figure 1.

Selective entry of a CD20-targeted MV in lymphoma cells from MCL patients. PBMC, including lymphoma cells, from three MCL patients (A, B and C) were infected with the CD20-targeted virus (MV-GFP H^{blind}antiCD20), the control virus with ubiquitous entry (MV-GFP), or left uninfected (shown only for patient A, left set of panels). Two days after infection CD45-positive live cells were gated, and among these cells CD20-positive and CD20-negative populations were identified (vertical axis). In each cell population, the percentile of GFP-expressing cells was determined (horizontal axis).

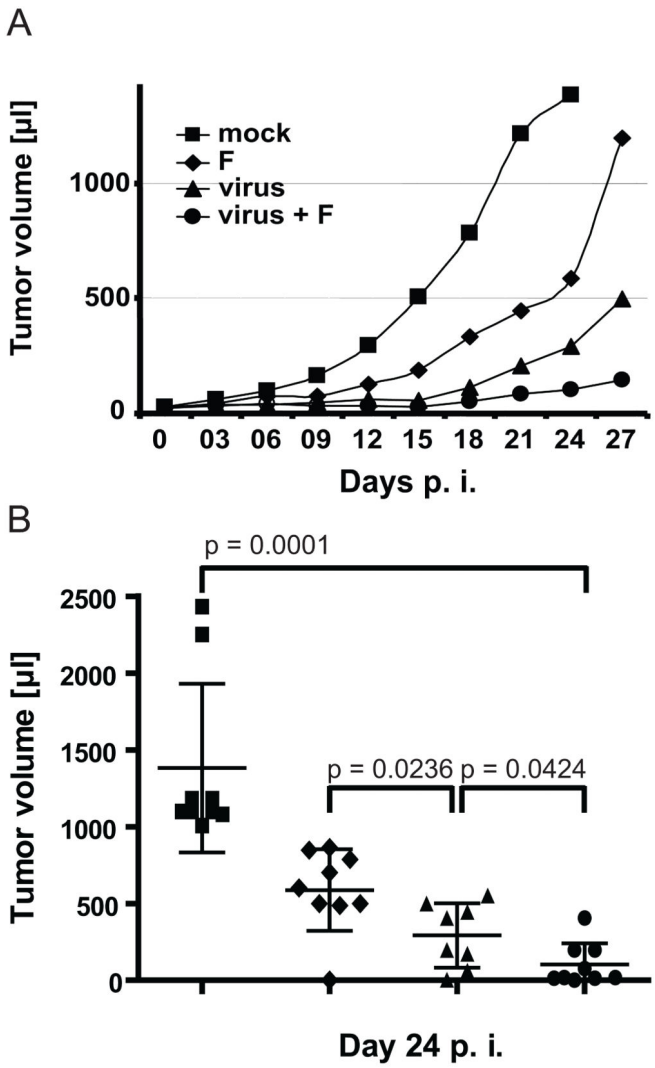

Figure 2.

Systemic treatment with virus and fludarabine reduces tumor burden. (A) Time course of tumor growth in four groups of 8–9 mice treated as indicated in the text. Curves are shown until the time when two mice in a group had to be sacrificed. (B) Tumor volumes of individual mice 24 days after the beginning of the treatment. The average tumor volume is indicated by an horizontal line; error bars indicate the standard deviation.

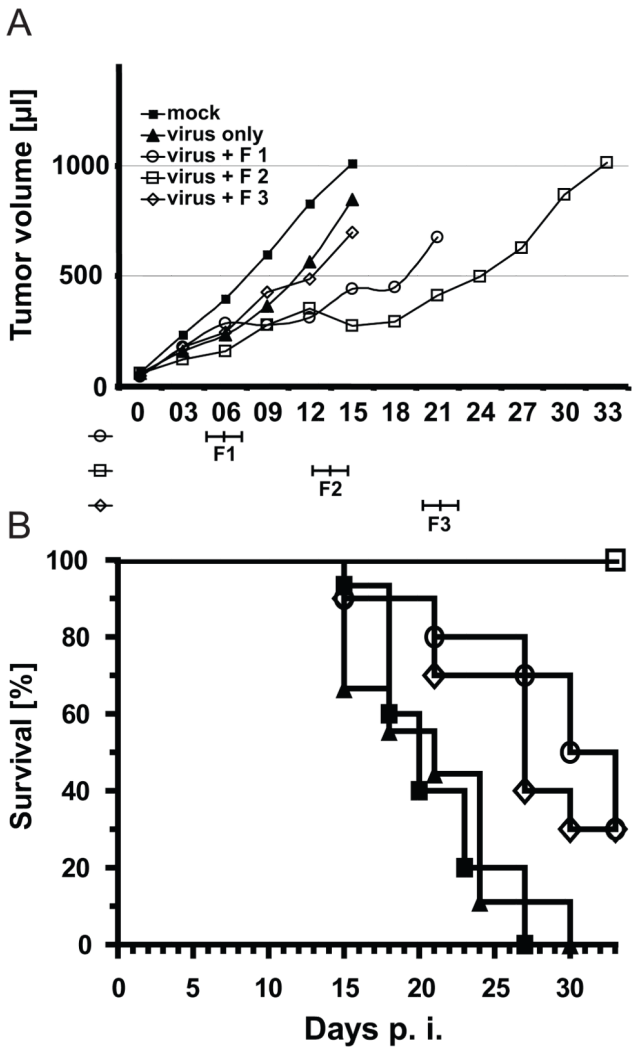

Figure 3.

Time course of tumor growth in mice treated with fludarabine at different intervals after virus delivery (A) and Kaplan Meier survival curve of the same mice (B). Groups of 9–11 mice were treated with fludarabine immediately after virus administration (F1), or after a one week interval (F2), or a two weeks interval (F3). In (A) curves are shown until the time when two mice in a group had to be sacrificed. In (B) the defined end point was a 1.5 ml tumor volume.

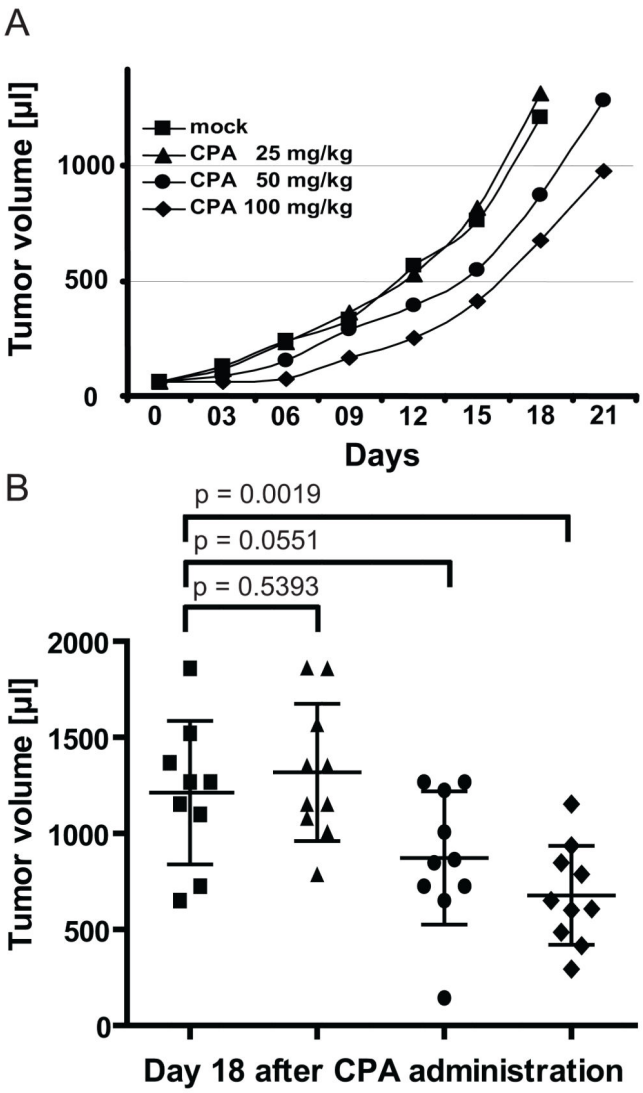

Figure 4.

Time course of tumor growth (A), and tumor volume at day 18 (B), in mice treated with different doses of CPA. Groups of 10 mice were treated with the three single doses of CPA indicated, or left untreated. Squares: mock-treatment. Triangles: 25 mg/kg CPA. Dots: 50 mg/kg CPA. Diamonds: 100 mg/kg CPA. The average tumor volume is indicated by an horizontal line; error bars indicate the standard deviation.

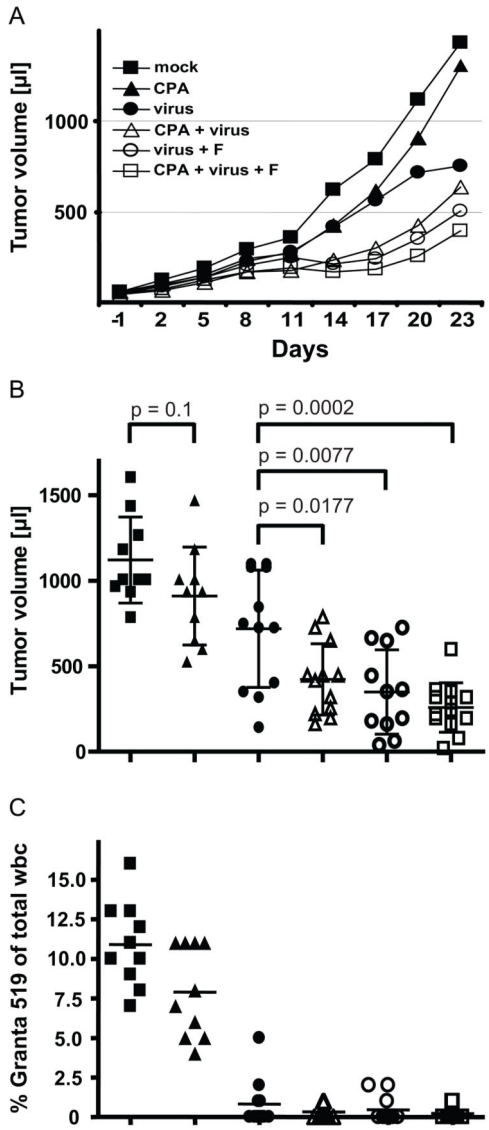

Figure 5.

Triple regimen chemovirotherapy. (A) Time course of tumor growth in mice treated with different combinations of CPA, virus and fludarabine. (B) Individual tumor volumes at day 20 after virus administration. Groups of 10–12 mice were treated. Timing of administration of the three treatments is as detailed in the main text. (C) Percentile of Granta cells in white blood cells (wbc) on day 25 after start of treatment. The six treatment groups are shown using the same symbols in each panel.

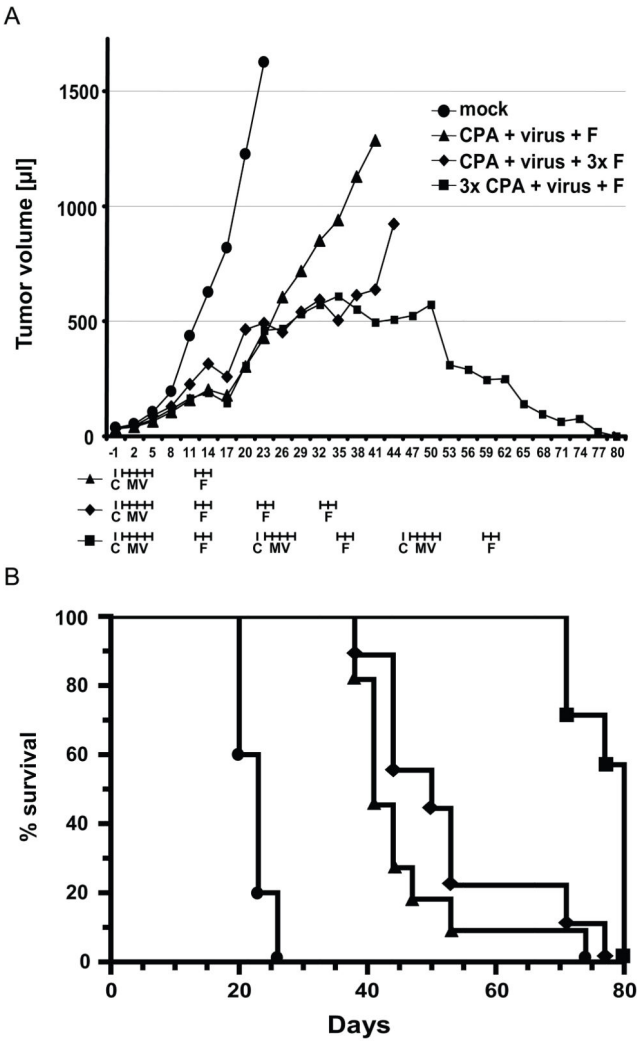

Figure 6.

Repeated sequential chemovirotherapy leads to complete regression of implanted tumors and long-term survival. (A) Time course of tumor growth in mice treated with different regimens of three therapeutics. Groups of about 12 mice were treated, but fatalities due to repeated injections caused some losses in each group, as detailed in Table I. The schedule of each treatment is indicated below the time axis. C: CPA. MV: measles virus. F: fludarabine. (B) Kaplan-Meier survival curves. Symbols are as in panel A. The defined end point was 1,700 µl tumor volume. After day 52, no mice had to be sacrificed because of excessive tumor volume.

Table I

Symptoms and pathology in individual mice

	Symptoms			Pathology				
Group (number of mice) *	**Wasting**	**Leg paralysis**	**Other adverse symptoms** **	**Number of mice at necropsy** †	**Average day of necropsy**	**Secondary tumors**	**Enlarged spleen** ‡	**Granta cells in blood at necropsy**
Control group (10 mice)	No mice	No mice	No mice	8	21.9	#33	All mice	All mice
Group 1 (11 mice)	#31,43,45	#29,45	#21,31,43	9	42.7	#29,44,45	#12,17,21,44,52	#12,17,21,44
Group 2 (9 mice)	#7,8,13,16,28	#7,16,28	#8	7	56	#8,25	#2,25,37,47	#2,37,47
Group 3 (7 mice)	#11,20,24,34,39,49	#39,49	#11,24,34,49	4	77.8	#11,24,34	No mice	#11,24,34

*Experimental groups included initially about 12 mice but some sudden treatment-related fatalities occurred, especially after IV injection of virus or control Opti-MEM. The number of fatalities was highest in group 3, in which each animal received multiple rounds of treatment.

**Other adverse symptoms included ascites, labored breathing, a hunched posture and body tremors.

†Some mice were not available for necropsy.

‡Enlarged spleen is defined as > 175% of the weight of age-matched normal SCID mice.